The Fine Guidance Sensors Aboard the Hubble Space Telescope, the Scientific Capabilities of these Interferometers

Edmund Nelan[a], Olivia Lupie[a], Barbara McArthur[b], G. Fritz Benedict[b],
Otto Franz[c], Larry Wasserman[c], Linda Reed[d], Russ Makidon[a],
Lauretta Nagel[a]

[a]Space Telescope Science Institute, Baltimore M
[b]University of Texas at Austin, Austin Texas,
[c]Lowell Observatory, Flagstaff, Az,
[d]Raytheon, Danbury Ct.

ABSTRACT

The Fine Guidance Sensors (FGS) aboard the Hubble Space Telescope (HST) are optical white light shearing interferometers that offer a unique capability to astronomers. The FGSs's photometric dynamic range, fringe visibility, and fringe tracking ability allow the instrument to exploit the benefits of performing interferometry from a space-based platform. The FGSs routinely provide HST with 2 milli-seconds of arc pointing stability. The FGS designated as the Astrometer, FGS3, has also been used to (1) perform 2 mas relative astrometry over the central 4 arc minutes of its field of view, (2) determine the true relative orbits of close (20mas) faint (m_v=15) binary systems, (3) measure the angular diameter of a giant star, (4) search for extra-solar planets, (5) observe occultations of stars by solar system objects, as well as (6) photometrically monitor stellar flares on a low mass M dwarf. In this paper we discuss this unique instrument, its design, performance, and the areas of science for which it is the only device able to successfully observe objects of interest.

Keywords: interferometry, astrometry, Koesters prism, FGS, binary stars, parallax, mass luminosity ratio

1. INTRODUCTION

The Hubble Space Telescope is well known for its superb images and spectroscopy. It is less well known as a space-based interferometer. Indeed, HST has not one but three interferometers onboard, the Fine Guidance Sensors (FGSs). The FGS is a clever solution to a fundamental dilemma, i.e., how is it possible to provide HST with 2 to 5 milli-seconds of arc (mas) pointing stability when HST is diffraction limited at about 40mas? An imaging device is certainly not the instrument of choice for this task, but a white-light shearing interferometer, such as the FGS, can meet this requirement. The fringe pattern of a guide star observed by the FGS provides HST's pointing control system (PCS) with simple, yet precise "fine error signals" used to measure and correct the small pointing errors of the spacecraft to maintain its attitude on the sky for prolonged exposures by the science instruments. The FGS is also well suited for use as a science instrument to study areas in astrometry and astronomy not possible by any other instrument or facility. In this paper we discuss the design of the FGS, its interferometric performance with HST's spherically aberrated wavefront, its operating modes, capabilities as a science instrument, and the areas of scientific investigations for which there is no alternative.

2. INSTRUMENT DESIGN

As an interferometer, the FGS is quite different from a long-baseline Michelson Stellar Interferometer. Long baseline interferometers determine the angle between a luminous object on the sky and the interferometer's baseline by measuring the difference in path length of the coherent beams collected by separated apertures. The FGS[1] measures the angle between a star and HST's optical axis by presenting the star's collimated and compressed light to a polariz-

ing beam splitter and a pair of orthogonal Koesters prisms. These prisms produce output beams with relative intensities dependent upon the angle between the wavefront's propagation vector and the entrance face of the prism.

Figure 1. FGS Field of View in the HST Focal Plane with FGS (x,y) Coordinate System Related to HST (V2,V3) System

.

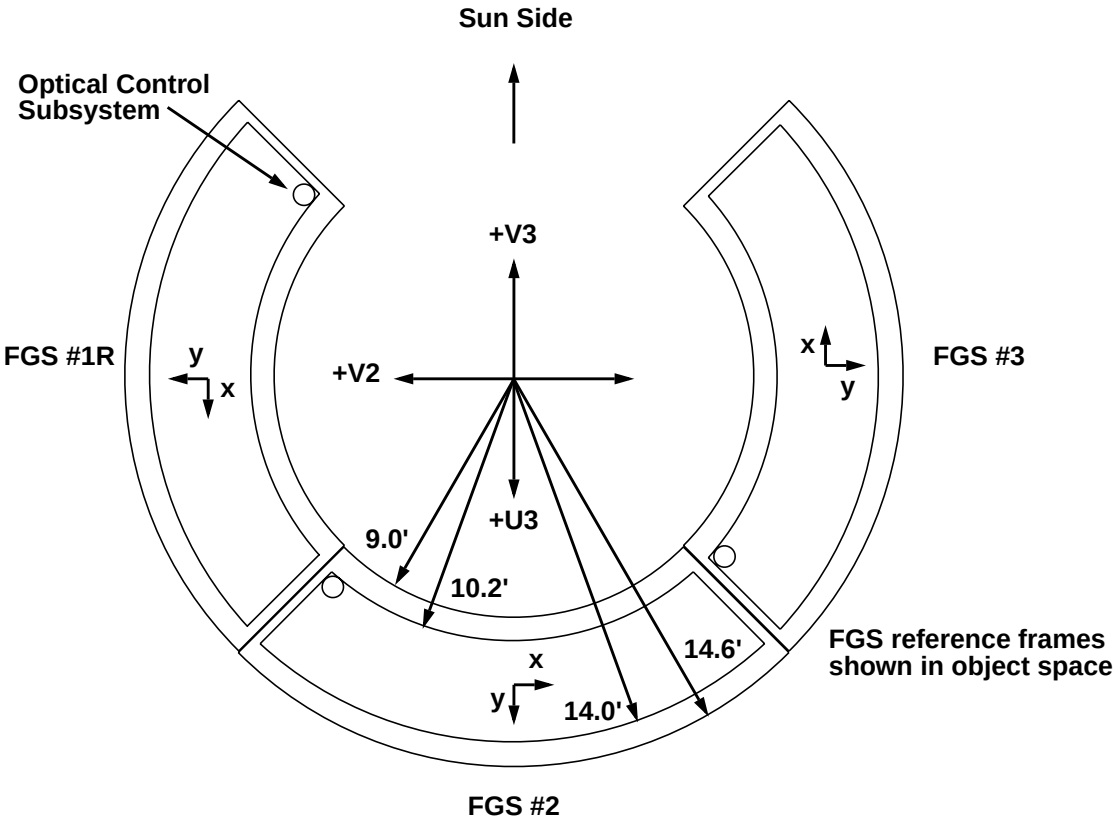

The FGS can acquire and observe any sufficiently bright object (m_v<17) over a 69 square arc minute field of view (FOV). Figure 1 shows the FGSs in HST's focal plane. The FOV is a quarter annulus at the outer perimeter of HST's focal plane with an inner and outer radius of 10 and 14 arc minutes respectively. However, only a 5x5 arc second (asec) aperture, the instantaneous field of view (IFOV), samples the sky at any one time. The location of the IFOV within the instrument's FOV (figure 2) is determined, with sub-mas precision, by a dual component star selector servo system (called SSA and SSB). Only the light from objects in this IFOV is presented to the polarizing beam splitter and Koesters prisms for interferometric fringe construction.

We describe the FGS as composed of two logical sub-systems, the "forward steering" section and the 2 orthogonal interferometers (figure 3). The forward steering component brings the IFOV to the desired location in the FOV. It is composed of a plane pickoff mirror which intercepts light from HST's optical telescope assembly (OTA) and redirects the beam into the FGS. The beam passes through focus and the encounters the Aspheric Collimating Mirror which collimates and compresses it (60x) to 42 mm. The beam next encounters the Star Selector Servo A assembly (SSA), a rigid assembly of two mirrors and a 5 element refractive corrector group which can be rotated about HST's optical axis (for reasons to be made clear below). The corrector group compensates for the design optical aberrations from both the OTA and the asphere. From the OTA come astigmatism and field curvature, while the asphere contributes astigmatism, spherical aberration, and coma. Unfortunately, the spherical aberration from HST's primary mirror is not corrected (it was, of course, not in the "design" to which the FGS was built!).

Figure 2: Locating the IFOV in the FOV

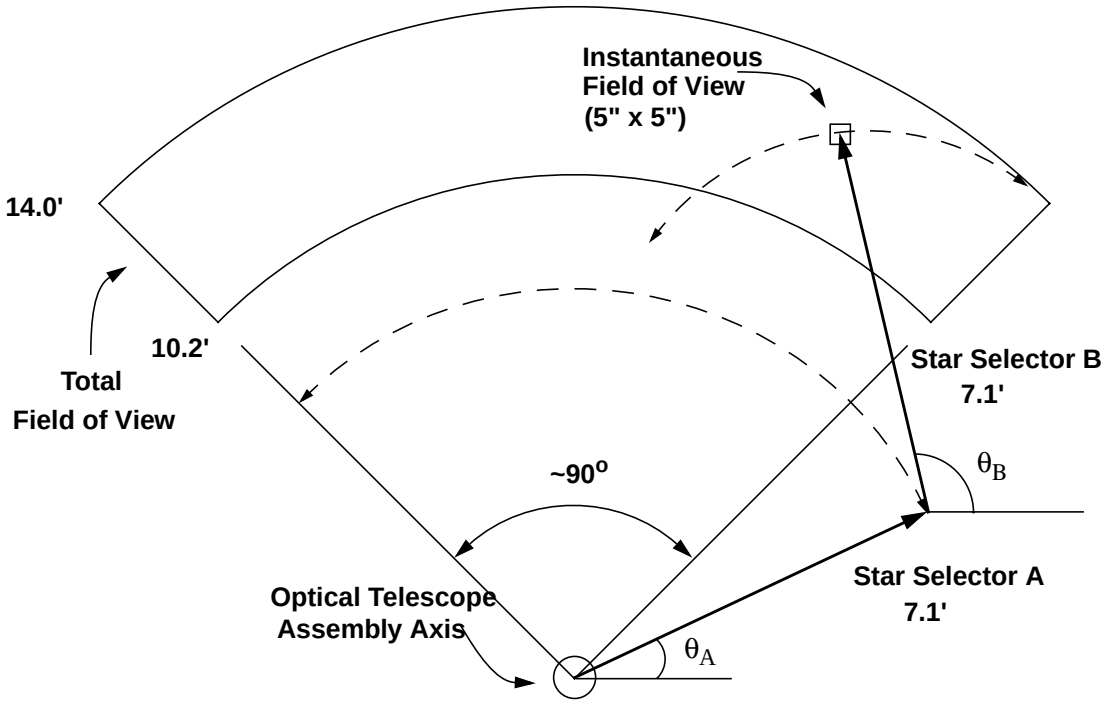

After exiting the SSA, the beam passes through a field stop which minimizes scattered light and narrows the IFOV. The beam next encounters the Star Selector Servo B assembly (SSB), which consists of a rigid assembly of four mirrors which, like SSA, can be rotated about an axis which is parallel to HST's optical axis. Upon exiting the SSB assembly, the beam encounters a fold flat mirror, the filter wheel assembly, another fold flat mirror, and finally the polarizing beam splitter.

The rotation angles of the SSA and SSB assemblies completely determine the location of the IFOV within the instrument's full FOV. Together, these assemblies transmit to the polarizing beam splitter only those photons originating from a narrowly defined direction, masking out all but a small 5x5 asec patch of sky (figure 2).

The polarizing beam splitter, the Koesters prisms and their associated field stops and photo-multiplier tubes comprise the interferometer section. The polarizing beam splitter divides the incoming unpolarized light into two linearly plane polarized beams with orthogonal polarizations, each having roughly half the incident intensity. Each beam is directed to a specific Koesters prism.

The pyramid shaped Koesters prism (figure 4) consists of two halves of fused silica joined along a surface coated to act as a dielectric beam splitter. By reflecting half the photons while transmitting the remainder, the dielectric performs an equal intensity division of the beam. This division also introduces a 90 degree phase difference, with the transmitted component lagging the reflected. This division and phase shift gives the Koesters prism its interferometric properties. The beam reflected from one side of the prism, when joined with the beam transmitted from the other side, constructively or destructively interfere to a degree which depends upon the angle between the incoming wavefront's propagation vector and the normal to the prism's entrance face in the plane perpendicular to the dielectric's surface. This angle is defined as the *tilt* of the wavefront. Thus, the Koesters prism emits two exit beams whose relative intensities depend upon the tilt of the incident wavefront. Each exit beam is focused by a positive doublet onto a photomultiplier tube (PMT) which records the number of photons encountered during a 25 msec interval.

Figure 3. FGS Optical Train

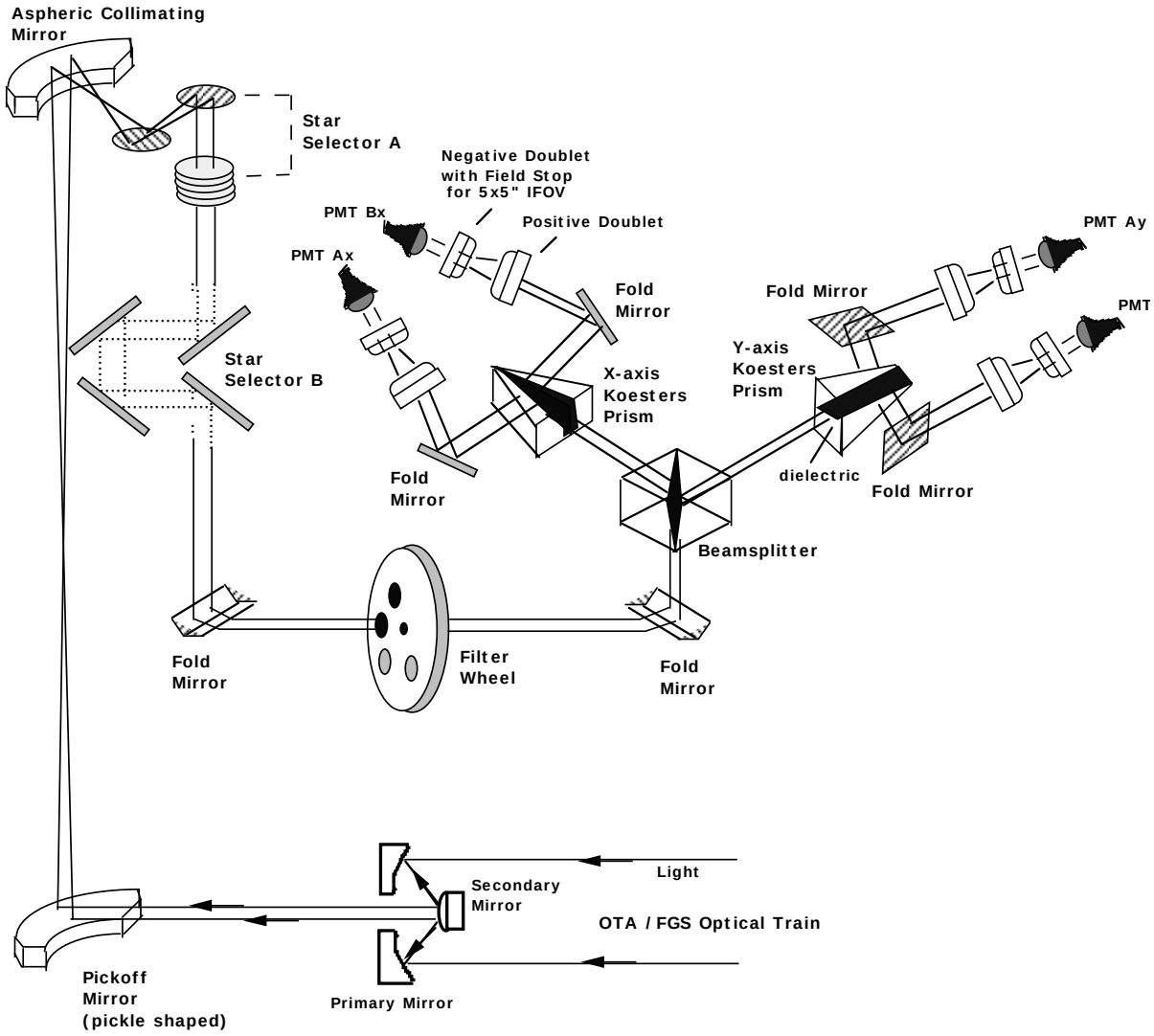

For the FGS to sense angular displacements in the plane of the prism's dielectric surface, another, orthogonally aligned Koesters prism is required. This prism intercepts the other beam emitted by the polarizing beam splitter.

Small rotations of the SSA and SSB assemblies alter the direction of the wavefront's propagation vector, and hence the tilt of the wavefront at the face of the Koesters prisms. Since the degree to which the transmitted and reflected beams within the prism constructively or destructively interfere with one another (and hence determine the intensity of the exit beams) depends upon the tilt of the incident wavefront, the PMT counts will vary as the SSA and SSB assemblies "scan" the IFOV across the object. By mapping the normalized difference of the PMT counts to the location of the IFOV for small tilts (less than 100 mas), the interferometer's fringe pattern emerges. Explicitly, if A is the number of photons recorded during a 25 msec interval by the "A" PMT on the FGS's x channel, and similar for B, then at every position of the IFOV, the fringe, or transfer function, is given by;

$$S = (A - B) / (A + B)$$

Figure 4. Koesters Prism and the incident wavefront. Tilt axis located at b.

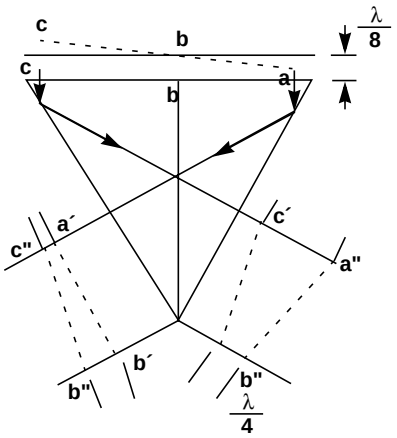

Figure 5. FGS3's interferometric response to a point source, the "S-curves"

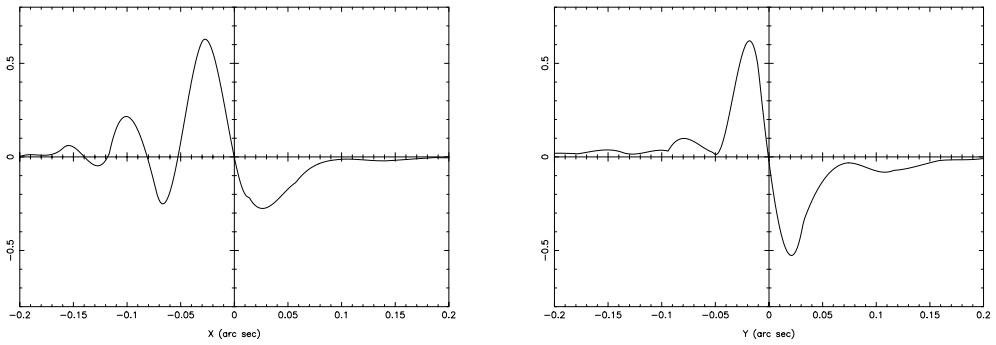

For large (> 100mas) wavefront tilts the photons constructively and destructively interfere at approximately the same rate, and S = 0 in the "wings" of the fringe.

This fringe pattern is referred to as the "S-curve" due to its characteristic morphology. Since the FGS is a 2-dimensional interferometer with two mutually orthogonal Koesters prisms, there will be two fringe patterns, one for the x-axis, the other for the y-axis. (The alignment of the FGSs in HST's focal plane, and hence the orientation of the interferometer's axis, is shown by figure 1.) Figure 5 displays the x and y-axis S-curves of FGS3. It is immediately obvious that they have distinctly different fringe amplitudes and morphologies, a result of the combined effects of HST's spherical aberration and small internal optical misalignment within FGS3.

3. SPHERICAL ABERRATION AND THE EFFECT ON THE FGS

In 1990, when the first HST images from the wide-field/planetary camera were analyzed, it was realized that the primary mirror was misfigured (the center of the mirror is too shallow with respect to the edges by about 230 microns) and that HST's wavefront is spherically aberrated. It was not yet appreciated that the FGSs would be affected in any way since the FGS collimates rather than focuses light. A collimated beam that is spherically aberrated results in a wavefront with curvature rather than one that is planar. Provided that the axis of rotation of the wavefront at the face of the Koesters prism is perfectly aligned (in the same plane) with the dielectric surface within the prism (point "b" in figure 4), the interferometric response would be unaffected by spherical aberration.[1, 10] However, small deviations

from perfect alignment result in the transmitted beam being recombined with a reflected beam with a small error in the phase, thereby affecting the interference process and subsequently decreasing the fringe's amplitude as well as deforming its morphology.

In orbit tests of the FGSs were made to evaluate the impact of the OTA's spherical aberration upon the instruments' performance. Four facts soon became clear. First, the amplitude and morphology of the S-curves from all three FGSs were degraded to various degrees. The fringes in both FGS1 and FGS2 were of such low amplitude that they would not be "visible" above the photometric noise from all but the brightest stars. Secondly, FGS3 displayed adequate fringe visibility over only the central third of its FOV (i.e., its performance is "field dependent"). Third, the FGSs, while guiding HST, would need to be operated with the 2/3 PUPIL stop in place. The PUPIL stop is a position in the FGS's filter wheel assembly that contains an aperture with a linear obscuration ratio of 2/3. This aperture essentially removes the contribution to the collimated beam originating from the outer 1/3 of HST's primary mirror, thereby reducing the effective phase error of the wavefront at the Koesters prisms. This improves the fringe visibility and morphology, but its use also masks out 50% of the source's photons, making the guide stars appear almost 1 magnitude fainter. Aside from increasing the photometric noise present in a star's fringe, it also disqualifies a significant number of potential candidates at the faint end of the guide star catalogue

Finally, it became clear that only FGS3 performed at a level suitable for use as a science instrument. It was thereby declared the Astrometer[3].

Despite the loss of performance inflicted upon the FGSs by HST's spherical aberration, all pre-launch requirements, both for guiding the telescope and astrometric measurements, have been met or exceeded, with the exception of FGS2's access to the faint end of the guide star catalogue.However, in mid 1996 it became apparent that FGS1 was increasingly vulnerable to mechanical failure, the bearings in its Star Selector A Servo assembly had worn to the point were the assemble would intermittently not rotate as commanded. Thus, FGS1 needed to be replaced during the 1997 Second Servicing Mission to HST.

4. **FGS1R**

Four FGSs had been built, three had been flown. The fourth remained in Danbury, Ct. with its manufacturer, then Hughes Danbury Optical Systems (HDOS), now Raytheon. Ground test stations had been modified to produce a spherically aberrated wavefront for a more realistic assessment of what to expect of an FGS's performance aboard HST. It was immediately apparent that the fourth FGS would suffer a loss of performance in a manner similar to the three in orbit. Christ Ftaclas, one of HDOS's optical experts, devised a method by which a critical optical component of a modified FGS could be re-aligned in orbit by command from the ground. The modification required the replacement of a stationary fold flat mirror with one mounted on an articulating mechanism. This, now referred to as the Articulating Mirror Assembly (AMA) replaced the fold flat #3 (FF3) mirror in the original design[10]. By adjusting the tip/tilt of the AMA, it became possible to re-align the wavefront's tilt axis with the Koesters prism's dielectric surface, thereby mitigating the deleterious effects of the spherical aberration.

The enhanced FGS, designed FGS1R (for replacement), was installed in HST in March 1997, replacing FGS1. Although the AMA had been adjusted before launch for optimal interferometric performance, in orbit evaluation of FGS1R's S-curves indicated a significant loss of performance, presumably due to the stress of launch and gravity release. Further studies indicated the misalignment was more likely due to motion of the Koesters prisms rather than a change in the orientation of the AMA. Early in the commissioning sequence, the AMA was adjusted to re-align the FGS and restore its interferometric fringes to near ideal.

The FGS team at the Space Telescope Science Institute (STScI), with support from the Raytheon, monitored the interferometer over the course of its first year in orbit. The fringe visibility on both axes showed continuous degradation, rapidly over the first three months, then more slowly. Stability seems to have occurred by about the 9th month. As of this writing, STScI, with support from Raytheon, plans to re-optimize FGS1R via AMA adjustment in early May, 1998, and then to conduct an angular resolution test to evaluate its performance as a science instrument.

Experience with FGS1R has illuminated three facts. First, the optical alignment of an FGS changes as a result of launch. Second, the alignments continue to evolve through most of the instrument's first year in orbit, presumably due to outgassing of the graphite epoxy composites upon which the optical bench is mounted. Third, an FGS confronted with a spherically aberrated wavefront requires an AMA to restore its interferometric performance after launch and time in space, regardless of how precisely it was aligned during the manufacturing process.

It is important to note that the FGS was not designed to operate with a spherically aberrated telescope. Had the wavefront been planar, pupil shifts on the order of 3mm, three times that experienced by FGS1R, would be well tolerated, the fringe visibility would be depressed by only about 10% and the S-curves would suffer no morphological degradations. This compares with a morphologically deformed S-curve with an 80% loss of fringe visibility with the spherical aberration (if 3mm pupil shift).

5. **OPERATING MODES OF THE FGS AS A SCIENCE INSTRUMENT**

To observe an object, the FGS must first acquire it. No other instrument onboard the Hubble Space Telescope can autonomously acquire and track a target. The other science instruments rely on HST's pointing control system (PCS), of which the FGSs are important members, to point the telescope so that the light from an object of interest enters the desired aperture. The FGS, on the other hand, relies on the spacecraft's computer only to place its IFOV in the vicinity of the object; thereafter it independently locates its target. To do so the FGS moves its IFOV along an outward spiral while monitoring the number of photons detected by the photomultiplier tubes (PMTs). Once a preset threshold is exceeded, the search is declared a success and the instrument then locates the target's photocenter by performing up to twenty 5 asec diameter circular nutations around the object.

At this point, the object is observed in one of two modes, POSITION or TRANSFER. In POSITION mode the FGS locates and tracks the object's interferometric fringes along both the x and y axis. This is useful for measuring parallaxes and proper motion of astrometrically interesting objects. In TRANSFER mode the FGS scans its IFOV across the object to fully sample its fringes. This mode has been extensively used with great success to study binary star systems with milli-second of arc accuracy.

POSITION MODE

To acquire the fringes of an object, the FGS offsets its IFOV a commandable distance from the target's photocenter along a 45 deg path in its x,y FOV coordinates, and then moves the IFOV towards it in 6mas (on the sky) steps along both axes. At each step the PMT counts are integrated for a specified amount of time, the FESTIME, which ranges from 25 msec for bright objects to 3.2 sec for faint objects. The absolute value of the normalized difference of the averaged PMT counts (referred to as the *fine error signa*l) are compared to a preset threshold. When the threshold is exceeded for three sequential steps, the FGS assumes the fringe has been located. From this point on, a continuous feedback loop between the Star Selector Servos and the fine error signal, recomputed every FESTIME, governs the repositioning of the IFOV. The FGS continuously adjusts the Star Selector positions by small rotations after every FESTIME interval in an attempt to set the fine error signal to zero, which analogues to the zero point crossing between the negative and positive peaks of the S-curve. In essence, the FGS attempts to keep the object's wavefront parallel to the entrance face of both the x and y axis Koesters prism.

Every 25msec the rotation angles of the Star Selector Servo assemblies and the four PMT counts are downlinked for post observation data analysis. In this way the object is precisely located in the FGS's FOV. After it has been tracked for a specified amount of time, typically 30 to 60 seconds, the spacecraft computer asserts control of the FGS and repositions its IFOV in the vicinity of the next object to be acquired and tracked. The entire process is repeated until all objects in the observation set have been observed.

The scientific goal of POSITION mode observing is to determine the relative angular separations between selected members of a specific star field. The FGS data yields precise locations of the stars in the instrument's FOV. Unfortunately, as a result of the FGS/HST optics and the star selector servo mechanisms, the FOV is distorted with respect to

the sky. These distortions, referred to as the Optical Field Angle Distortions (OFAD) are as large as 500 mas but are calibrated at the 1 to 2 mas level and thus can be removed from the data[5].

Another correction needs to be made for differential velocity aberration. This is the apparent change in the angle between an object in the telescope's focal plane and the velocity vector of the spacecraft as a function of HST's velocity in the barycentric rest frame. Since the aberration varies with position in the focal plane by an amount which is astrometrically large, up to 30mas, it must be and is accounted for in the data reduction process[5,6].

A third source of error, which had been entirely unanticipated, is the apparent drift of the FOV across the sky during an observing sequence. In a typical observation set as many as 12 individual stars are observed, and a select few, those designated as *check stars*, are observed several times at more or less uniformly spaced intervals. These check stars are often seen to drift in the FOV from one measurement to the next, an effect not witnessed by the two guiding FGSs. (It should be pointed out that the guide stars also drift in the guiding FGSs, but this is interpreted as a pointing error. The spacecraft's pointing control system re-points HST to remove the "error", which in effect removes the apparent drift of the guide stars. This re-pointing is, of course, witnessed by the astrometer FGS.) The apparent rate and direction of the drift correlates well from one check star to the next. The origin of the drift is not well understood, i.e., it is not clear as to whether it arises from small focus changes of the OTA or from thermal cycling of the FGS. The drift can be as large as 30 mas, but since it is generally well behaved, it is easily modeled and removed from the data during post observation processing[5,6].

Once all of the calibrations have been applied, the per-observation relative angular separations of stars brighter than about m_v=15 measured by the FGS in POSITION mode are accurate to about 1 to 2 mas[4]. For stars as faint as m_v=17 (the FGS's faint magnitude limit) the accuracy is about 3 mas. These errors include both statistical and systematic components. Repeated measurements can, of course, reduce the statistical errors but are no help in addressing the systematic contributions, of which the OFAD is dominant. The overall accuracy of FGS relative astrometry in POSITION mode is on the order of 1.5mas for objects observed in the central third of the FOV. Outside this restricted region the OFAD calibration becomes less reliable and the instrument's astrometric accuracy degrades to as high as 3mas.

Pre-launch expectations of FGS astrometry called for 2.7mas accuracy. FGS3, operating in the light of a spherically aberrated telescope, subject to drifts of its FOV across the target field as large as 30mas, and optical field angle distortions of typically 500 mas, has exceeded this requirement for objects as bright as m_v=7 and for those as faint as m_v=16. Its performance in TRANSFER mode, however, has been even more impressive.

TRANSFER MODE

In TRANSFER mode an object is initially acquired in the same way as in POSITION mode, but instead of locating and tracking the fringe, the FGS's IFOV is "scanned" across the object's photocenter to sample the entire fringe pattern. In effect this moves the IFOV across the sky in the vicinity of the star, thereby changing the tilt of the wavefront on the faces of the Koesters prisms and modulating the number of photons recorded by each of the four PMTs. Every 25 msec the Star Selector Servo rotation angles and the PMT data are downlinked. The instantaneous position of the IFOV can be determined from the Star Selector data, while the fringe pattern can be reconstructed from the PMT data and mapped against the IFOV's position. The "length" of the scan, the size of the angular sweep of the IFOV on the sky, is typically 1" to 2". The resolution of the fringe, or "step size" of the scan, is usually 0.6mas. To achieve adequate signal to noise in the post observation reconstruction of the fringe pattern, multiple scans, up to 30, are made in a given observation and are coadded and averaged[2].

Transfer mode observing is used to study binary star systems[7] as well as to determine the angular size of the disks of resolvable giant stars. The light from one member of a binary system is mutually incoherent with that from the other since it originates from a different direction on the sky. Since light from two incoherent sources cannot interfere, the effect, in TRANSFER mode, is the linear superposition of the two point source fringe patterns, each scaled

Figure 6. The effect of binaries on the FGS3 y-axis S-curveS

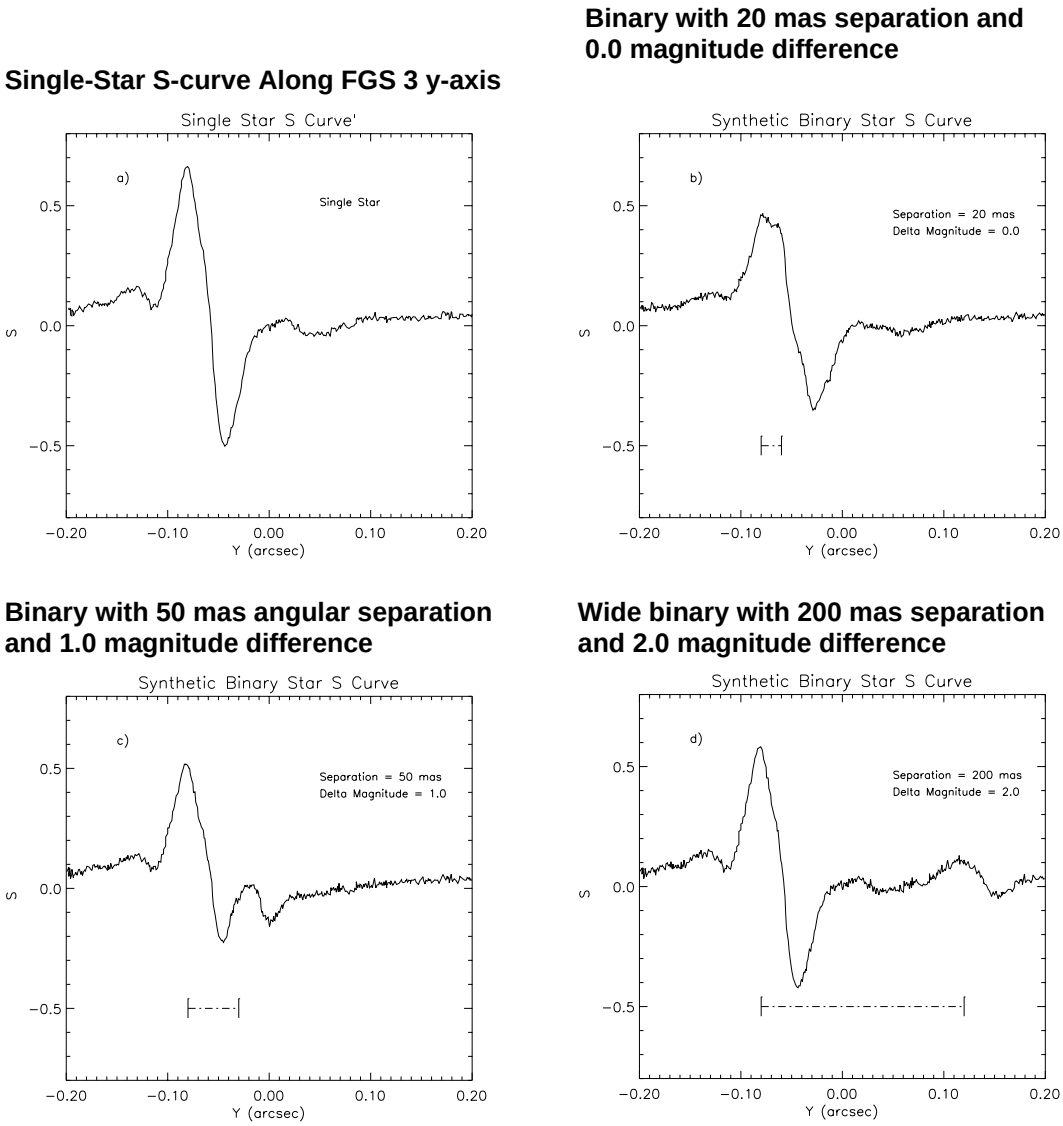

by the relative brightness of the sources and shifted by an amount which correlates with the angular separation of the binary's components. The composite fringe pattern, S_b, will be given by;

$$S_b(x) = l_1 * S(x) + l_2 * S(x+d)$$

where S(x) is the point source S-curve at wavefront tilt angle x, l_1 / l_2 is the relative brightness of the components, constrained by $l_1 + l_2 = 1$, and d is the projected angular separation along this axis of the interferometer.

For example, if one star in a binary system is twice as bright as the other and they are separated by 300 mas, which is wider than the FGS's fringe, the result is two S-curves, separated by 300 mas, with one having twice the amplitude of the other. The amplitude of the bright star's S-curve will be 2/3 that of a point source since the light from the com-

panion acts as a background in the interference process the brighter star. (Of course, the light from the bright star acts the same way upon the fringe of the fainter star.) Figure 6 demonstrates the effect of double stars on the FGS's fringe pattern.

The dual fringes from a binary star system need not be well separated (distinct) for post observation data analysis to succeed at determining the angular separation and relative brightness of the components. In FGS3, with near ideal fringes along the interferometer's y-axis, TRANSFER mode observations of binaries with projected angular separations as small as 10 mas have been successfully performed. The real limiting factor, for FGS3, is the x-axis, where the point source fringe visibility is not only reduced to 67% of its ideal value but is also morphologically deformed, as seen in figure 5. Along this axis, angular separations of less than 20 mas are generally not measurable.

The FGS in TRANSFER mode has been successfully used[8] to study binary systems with a total brightness as faint as m_v=15, components separated by as little as 30mas, and relative magnitude differences as large as 3. It is anticipated that FGS1R will out perform FGS3 by being able to measure angular separations perhaps as small as 7 mas (provided the system is brighter than m_v=14.5 and the magnitude differences are less than 2). In early May 1998, STScI will test FGS1R's performance by varying the projected angular separation of the components of a binary system along one of the interferometer's axis by rolling the telescope with respect to the binary's position angle. Projected separations to be tested are 6, 8, 10, 12, 15 and 20 mas. To learn more about the outcome of this test, interested readers are encouraged to consult the FGS web page at

http://www.stsci.edu/ftp/instrument_news/fgs/html.

6. CONCLUSIONS

The Hubble Space Telescope's FGS astrometry program offers astronomers the means to measure the parallax and proper motions of objects as faint as m_v = 16 over several arc minute fields with accuracies often better than 2 mas. The FGS can also resolve the components of faint (m_v= 15) binary systems with magnitude differences as large as 3 and separations as small as 20 mas (and less with FGS1R) at an accuracy of about 1 mas. By simultaneously observing binary systems in TRANSFER mode along with reference stars in POSITION mode, the observer can determine the true relative orbit as well as measure the object's parallax. With these data, the system's total mass can be determined. If the astrometry is of sufficient quality, the motion of each component about the system's barycenter can be measured, which in turn, yields the relative masses. When this is coupled with the photometric data, the mass to luminosity ratio of each component becomes known. This technique has been successfully applied to observe a low mass binary system[9].

On the other hand, if a double lined spectroscopic binary (a two component radial velocity object) is observed with the FGS in Transfer mode at an adequate number of points along its orbit, then the true parallax of the object can be determined without needing to resort to positional astrometric measurements.

No imaging device is available to study the small separation binary systems observable by the FGS. The ground based long baseline interferometers can resolve objects where even the FGS would fail, but only if the object is bright (m_v<6) or is within (typically) 30" of a bright star (for active fringe tracking). Speckle interferometry can observe objects as faint as m_v=11 but provides no differential photometry and cannot resolve structure below 30 mas (even then, not with the 1mas accuracy of the FGS). Even with the expected advances in ground based long baseline interferometers (e.g., Keck, VLTI)[11], it appears that the FGS will be unchallenged as the only instrument available for the study of binary systems fainter than about m_v = 8 and separations less than 40 mas. This, along with its ability to simultaneously provide 1-2 mas relative astrometry for these objects, provides the FGS with a niche occupied solely by itself, probably until the arrival of the long baseline interferometers in space, such as SIM in 2005.

7. REFERENCES

1. O. Lupie, E. Nelan, R. Makidon, L. Nagel, 1998 FGS Instrument Handbook, Version 7.0, STScI, Baltimore Md.

2. 1997 HST Data Handbook, Version 3.0, Volume I, M.Voit, ed., STScI, Baltimore, Md.

3. G. F. Benedict, E. Nelan, D. Story, B. McArthur, A.L. Whipple, W.H. Jefferys, W. Van Altena, P.D. Hemenway, P.J. Shelus, O.G. Franz, L. Wasserman, A. Bradley, L.W. Fredrick, R.L. Duncombe, "Astrometric Performance Characteristics of the Hubble Space Telescope Fine Guidance Sensors", PASP **104**, 958, 1992

4. G.F. Benedict, B. McArthur, E. Nelan, D. Story, A. Whipple, "Astrometey with HST FGS3, POSITION Mode Stability and Accuracy", PASP, **106**, 327, 1994

5. B. McArthur, G.F. Benedict, W.H. Jefferys, and E. Nelan, "Maintaining the FGS3 Optical Field Angle Distortion Calibration", in Proc. 1997 HST Calibration Workshop, ed. S. Casertano, R. Jedrzejewski, T. Keys, and M. Stevens, STScI publications

6. E. Nelan, O. Lupie, L. Nagel, "Astrometry with the FGS in POSITION Mode and TRANSFER Mode: Observing Strategies, Pipeline Processing and Data Reduction", in Proc. 1997 HST Calibration Workshop, ed. S. Casertano, R. Jedrzejewski, T. Keys, and M. Stevens, STScI publications

7. O. Franz, L. Wasserman, A.J. Bradley, G.F. Benedict, R.L. Duncombe, P.D. Hemenway, W.H. Jefferys, B.McArthur, E. Nelan, P. Shelus, D. Story, A.L. Whipple, L.W. Fredrick, W. van Altena, "astrometric Companions Detected at Visible Wavelengths with the Hubble Space Telescope Fine Guidance Sensors" BAAS, **185**, 85.24, 1994

8. O. Franz, 81st Meeting of the Space Telescope Astrometry Team, University of Virginia, Charlottesville, Va. 1998

9. J. Hershey, L. G. Taff, in preparation

10. K.P. Chisholm, C. Ftaclas, L. Abramowicz-Reed, "On-orbit Performance of the Fine Guidance Sensor-1R", 1998 SPIE Symposium on Astronomical Telescopes and Instrumentation, Proceedings, Conference 3350-126.

11. Various Contributions, 1998 SPIE Symposium on Astronomical Telescopes and Instrumentation, Proceedings, Conference 3350.